Ultrastructural Characteristics of Carcinogen-Induced Dysplastic Changes in Tracheal Epithelium

A. J. P. Klein-Szanto, MD, D. C. Topping, PhD, C. A. Heckman, PhD, and Paul Nettesheim, MD

Squamous metaplasias with various degrees of atypia, carcinomas *in situ*, and microinvasive carcinomas produced in rat tracheal transplants by a 4-week exposure to dimethylbenz(*a*)anthracene were studied 12–96 weeks after cessation of carcinogen exposure. In addition to the classical nuclear and cytoplasmic indicators of atypism, the squamous metaplasias with slight and moderate atypia were characterized by the presence of glycogen in the spinous layer, atypical composite keratohyalin granules in the granular layer, and in most cases an orthokeratinized horny layer. The squamous metaplasias with severe atypia showed an increased secretory activity and a decreased number of desmosomes. Carcinomas *in situ* were characterized by numerous intracellular and extracellular microcysts filled with secretory material identified by histochemical techniques as containing neutral glycoproteins and sialomucins. Microinvasive carcinoma showed similar characteristics, with an increase in polylobulated nuclei and appearance of multilaminar ergastoplasm. An outstanding feature in all these lesions was the presence of dark fusiform epithelial cells. They were observed in the middle layers in the squamous metaplasias with severe atypia and appeared in all layers of the carcinomas *in situ*. (Am J Pathol 98:83–100, 1980)

SQUAMOUS METAPLASIAS with varying degrees of atypia and carcinomas *in situ* (CIS) are generally regarded as immediate precursor lesions of invasive carcinoma.[1,2] We have found that the tracheal transplant model has been extremely useful for producing the whole range of precursor lesions. Furthermore, the lesions can be produced by brief measured exposures to chemical carcinogens. In this way epithelial changes can be analyzed many months after the acute effects subside, thus avoiding superposition of early toxic and carcinogenic effects. In parallel studies the fate and interrelationship of carcinogen-induced epithelial changes were described.[3,4] In the preceding paper we described the nondysplastic epithelial alterations observed in this experimental model.[5] In this report we describe the major characteristics of the advanced epithelial lesions of the tracheal mucosa, presenting varying degrees of dysplastic changes, emphasizing, when possible, the differences between the several stages encountered through the scale of epithelial alterations, ranging from the

From the Biology Division, Oak Ridge National Laboratory, Oak Ridge, Tennessee.

Supported by the National Institute of Environmental Health Sciences under Interagency Agreement Y-1 CP 50200 and the Office of Health and Environmental Research, US Department of Energy, under contract W-7405-eng-26 with the Union Carbide Corporation.

Accepted for publication July 23, 1979.

Address reprint requests to Dr. A. J. P. Klein-Szanto, Biology Division, Oak Ridge National Laboratory, P.O. Box Y, Oak Ridge, TN 37830.

0002-9440/80/0109-083$01.00

minimal morphologic deviation to the most advanced stage of invasive carcinoma.

Materials and Methods

The materials and methods used in this study are similar to those described in the accompanying report.[5] Briefly, rat tracheas were transplanted subcutaneously to the dorsum of syngeneic hosts. After a recovery period of approximately 4 weeks, these grafts were exposed to 165 or 200 μg dimethylbenz(*a*)anthracene (DMBA). After an exposure time of 4 weeks, the pellets containing the chemical carcinogen were removed from the grafts. Groups of 4 to 8 tracheal transplants were harvested at 12, 16, 24, 48, and 96 weeks after the cessation of carcinogen exposure. Most of the specimens used in the present study originated from the 16- and 24-week groups. The tissues were processed for electron-microscopic observation. An additional two groups harvested at 16 and 20 weeks were processed for light-microscopic observation and stained with periodic acid-Schiff (PAS) alone, with and without amylase digestion, and PAS followed by alcian blue (AB) staining at either pH 2.6 or pH 1. At least five specimens of each type of lesion were studied by light and electron microscopy.

Results

Grading of atypical lesions of respiratory mucosa has been carried out following the criteria and definitions currently applied to the equivalent alterations of most covering epithelia.[6–9] The main categories to be analyzed include squamous metaplasias with slight, moderate, and severe atypia (all of these lesions are sometimes referred to in the literature as dysplasias), CIS, and microinvasive squamous carcinomas.

All types of squamous metaplasias with atypia were characterized by recognizable stratification with or without orthokeratinization, increased mitotic figures, occurrence of atypical mitosis, variability in cellular size, shape, and stain affinity, as well as individual cell keratinization in the deeper layers (dyskeratosis). The histologic differences between these three types of dysplasias were mainly quantitative: the squamous metaplasias with slight atypia (Figure 1) showed a minimum of these alterations, the severe ones presented most of them (Figure 2), and those with moderate atypia exhibited an intermediate pattern. Although some squamous metaplasias presenting slight and moderate atypia (mainly the orthokeratinized cases) were also observed during the first 3 months, most epithelial alterations were seen late in the course of the experiments (12 to 48 weeks). No clear time-related distribution of lesions could be detected during this later period, although most advanced lesions were found around 16 and 24 weeks after the cessation of carcinogen exposure. Acid and neutral mucosubstances could be detected in all types of lesions, but they were scarce or absent in most orthokeratinized epithelia presenting slight and moderate atypia. The acid mucosubstances were noted with the PAS–AB (pH 2.6) stain and only slightly or not at all with the same

stain at pH 1. Several orthokeratinized lesions exhibited moderate amounts of amylase-sensitive PAS-positive material (Figures 3 and 4). The presence of glycogen was confirmed at the ultrastructural level (Figure 5). Electron microscopy showed that milder epithelial alterations had many features in common with the typical squamous metaplasias.[5] Although polymorphism was evident in some nuclear profiles and nucleolar patterns, many typical features were maintained, especially the differentiation gradients of tonofilaments, membrane-coating granules, and keratohyaline granules (KHs). Although individual KHs showed a normal distribution in the granular layer, they occasionally exhibited irregular and composite morphologic features [10] (Figures 6–8), and KH-like material was frequently found in the cell periphery (Figure 7). Secretory granules and abundant Golgi–endoplasmic-reticulum–lysosome complexes (GERL) were also frequently observed, especially in the middle and superficial layers. The presence of dark and clear basal epithelial cells, as well as the occasional absence of the basal lamina, although observed in regular squamous metaplasias, became much more apparent in the present group of lesions. A salient feature of these lesions, which could be recognized in 1-μ thick Epon sections stained with toluidine blue (Figure 1), was the presence of dark epithelial cells. These cells were characterized by a fusiform shape, elongated nuclei with condensed chromatin, electron-dense cytoplasmic matrix with abundant and closely packed organelles, and cytoplasmic filaments.

The squamous metaplasias with severe atypia, although still showing stratification, were rarely keratinized and frequently presented deep connective tissue papillae penetrating the epithelium (Figure 2). The presence of nonepithelial cells, especially histiocytes, was noted in several cases. Centralization, or margination of tonofilaments, and to a lesser extent total cellular dyskeratosis, as well as pleomorphic giant mitochondria, were observed in the basal and middle layers (Figure 9). The presence of dark epithelial cells in layers other than the basal layer (Figure 10) and irregularities of the basal lamina were frequent features.

The CIS were characterized by the absence of organized stratification, although in some cases the most superficial layer presented some flattened cells. Absence of cell polarity throughout the epithelium was a distinctive characteristic. Cell and nuclear abnormalities, such as dyskeratosis, pleomorphism, and atypical mitosis, were similar to those seen in invasive carcinomas. In the superficial layer intercellular or intracellular microcysts were frequently observed (Figures 11–13). The PAS–AB (pH 2.6) stain detected the presence of acid mucosubstances in these microcavities (Figure 12). The same histochemical stain at pH 1 was negative. Ultrastructural evidence of an active secretory function was observed in most cells, many

of which contained membrane-bound droplets compatible with mucus granules (Figure 13). Pleomorphism and atypia reached maximal expression, dyskeratotic cells were seen in all layers (Figure 14), and desmosomes were less numerous. Dark epithelial cells were seen in the basal and in all other layers (Figure 15). The basal lamina was intact in most areas, although interruptions were not unusual (Figure 14).

The atypical features that characterized the CIS were also seen in the early invasive carcinomas (Figures 16–18), although a higher tendency towards squamous differentiation was evident in most of the invading tumor tissue (Figure 16). On the other hand, characteristics such as highly lobulated or fragmented nuclei and multilaminar endoplasmic reticulum (Figure 18) were not seen in lesions other than invasive carcinomas. Active secretion and neutral and acid mucosubstance production, as shown both by positive PAS–AB (pH 2.6) staining and secretory cytoplasmic droplets detected by electron microscopy, were common features of many tumor cells.

Discussion

Electron-microscopic observation of atypical tracheal epithelial lesions showed that it is possible to detect a continuum of changes from the mildest to the severest alteration. This confirms the impression also obtained from the light-microscopic examination of such lesions.

Although many ultramorphologic modifications not detectable by light microscopy were observed, it was difficult to differentially characterize each of the epithelial alterations by descriptive electron microscopy. Most of the pathologic characteristics could be observed in all the lesions under study, and it was evident that the main difference between the several types of lesions was to a large extent quantitative. On the other hand, while comparing polar situations, such as squamous metaplasia with slight atypia and carcinoma, obvious morphologic differences were recognized.

The most prominent features common to all dysplastic lesions, including carcinomas, were irregularity of size and shape of both cells and nuclei, increased nucleolar size, nuclear invaginations and lobulation, alterations in tonofilament bundle distribution, dyskeratosis, pleomorphism of organelles, especially mitochondria, the presence of dark epithelial cells mainly in the basal layer, and the absence and/or duplication of basal lamina. Many of these features have been described in other preneoplastic and neoplastic conditions,[11] such as those produced in rodent airways by treatment with chemical carcinogens.[12–14] These characteristics, although found in all dysplastic and neoplastic lesions, occurred more frequently in the most advanced lesions.

The most outstanding feature observed in all these lesions was the presence of dark epithelial cells, which were observed in most layers in increasing numbers as the lesions became more and more severe. They probably constitute a cellular element closely linked with increased and/or disorderly proliferation, although they were also observed in normal epidermis [15] and in the regular squamous metaplasias without light-microscopically detectable atypia.[5] The dark epithelial cells of tracheal epithelial lesions, as well as those observed in promoter-treated epidermis, actively incorporated ^{3}H-thymidine,[16,17] providing an argument against the possibility of their being inactive or necrobiotic cells.

Some ultrastructural characteristics appeared almost exclusively in certain types of epithelial alterations. The squamous metaplasias with slight and moderate atypia were characterized by the presence of glycogen and in most cases presented an orthokeratinized horny layer. Atypical KHs were observed in the granular layer. The squamous metaplasias with severe atypia rarely presented a horny layer, showed an apparent decrease in desmosomes, and were characterized by the presence of dark epithelial cells in the basal and the middle layers. CIS were characterized by dark epithelial cells in all layers as well as a decrease in the number of cell junctions, especially desmosomes. Numerous intracellular and intercellular microcysts containing secretory material and other evidence of mucus secretion were very conspicuous. Some of these features seem to be related to a shift from a predominantly stratified squamous type of differentiation, characteristic of the milder lesions, to a predominantly secretory or mucous type of differentiation,[18,19] as seen in the more advanced lesions. The invasive carcinomas, although showing secretory characteristics in some cases, always exhibited a clear squamous differentiation. The ultrastructural evidence of secretory activity seen in the more advanced lesions, such as the presence of cytoplasmic secretory droplets, large Golgi complexes, prominent rough endoplasmic reticulum, and hypertrophic nucleoli, although not as conspicuous, was noted also in the less advanced epithelial alterations. Neutral and acid mucosubstances were detected by histochemical means in all dysplastic and neoplastic lesions. The acid mucosubstances seem to be composed mainly of sialomucins with very few or no sulfomucins as evidenced by the weak or absent positivity of the PAS–AB (pH 1) stain. These features seem to confirm the results from other models that imply that the mucous cell plays a very important part in the histogenesis of respiratory neoplasia.[14,20]

In contrast with Becci's finding [14] in the hamster showing glycogen in the CIS, we only detected amylase-sensitive PAS-positive material in the orthokeratinized squamous metaplasias with slight or moderate atypia. In

addition to the classical histopathologic features, CIS and microinvasive carcinoma showed few specific ultrastructural alterations. Apart from the extreme disorganization and lack of stratification, CIS exhibited in an exacerbated fashion ultrastructural and histochemical features similar to those of the squamous metaplasias with severe atypia. The same can be said about microinvasive carcinoma, which, although exhibiting an increased tendency towards squamous differentiation, presented many similarities with less advanced alterations. The presence of multilaminar endoplasmic reticulum in mitotic and interphase cells appears to be an exception. This abnormal endoplasmic reticulum configuration has been reported in other malignant and hyperplastic cells undergoing mitosis [21,22] and its presence in interphase points to an alteration in the division process.

The present ultrastructural analysis of dysplastic and neoplastic alterations of the tracheal epithelium has defined the characteristics of these important groups of lesions. This analysis has demonstrated that the major differences between the groups are quantitative rather than qualitative, especially when closely related alterations are compared. On the other hand, when the extremes of the spectrum of lesions are compared, obvious qualitative as well as quantitative differences are easily detected.

In a parallel study conducted in our laboratory employing a larger sample size, a chronologic evolution of morphologically less severe appearing lesions into those which are more atypical has been shown.[4] This is in accordance with what is known from other experimental and human data.[23,24] These facts increase the importance of an accurate determination of the degree of atypia that can be established with a good approximation using morphologic methods alone but that could be perfected to a considerable extent by the use of less subjective criteria derived from growth kinetics and histometric measurements. Some morphometric and cell kinetics parameters are being studied in our laboratory and will be the subject of a future report.[16]

References

1. Stenbäck F: Morphologic characteristics of experimentally induced lung tumors and their precursors in hamsters. Acta Cytol 17:476–486, 1973
2. Nettesheim P: Precursor of bronchogenic carcinoma. Cancer Res 36:2654–2658, 1976
3. Topping D, Nettesheim P: Quantitative assessment of sequential epithelial changes in tracheal mucosa following exposure to DMBA. Cancer Res (In press)
4. Topping D, Nettesheim P: Development and fate of focal lesions in tracheal mucosa following carcinogen exposure. Cancer Res (In press)

5. Klein-Szanto AJP, Topping DC, Heckman CA, Nettesheim P: Ultrastructural characteristics of carcinogen-induced nondysplastic epithelial changes in tracheal epithelium. Am J Pathol (Submitted for publication)
6. Reagan JW, Wentz WB: Genesis of carcinoma of the uterine cervix. Clin Obstet Gynecol 10:883–921, 1967
7. Pindborg JJ: Oral leukoplakia. Aust Dent J 16:83–93, 1971
8. Bauer WC, MacGavran MH: Carcinoma in situ and evaluation of epithelial changes in laryngopharyngeal biopsies. JAMA 221:72–75, 1972
9. Mukada T, Sasano N, Sato E: Evaluation of esophageal dysplasia by cytofluorometric analysis. Cancer 41:1399–1404, 1978
10. Jessen H: Two types of keratohyalin granules. J Ultrastruc Res 33:95–115, 1970
11. Bernhard W: Ultrastructure of the cancer cell, Handbook of Molecular Cytology. Edited by A Lima de Faria. Amsterdam, North-Holland Publishing Co., 1969, pp 687–715
12. Gould VE, Wenk R, Sommers SC: Ultrastructural observations on bronchial epithelial hyperplasia and squamous metaplasia. Cancer 28:426–436, 1971
13. Harris CC, Sporn MB, Kaufman DG, Smith JM, Jackson FE, Saffiotti U: Histogenesis of squamous metaplasia in the hamster tracheal epithelium caused by vitamin A deficiency or benzo(a)pyrene-ferric oxide. J Natl Cancer Inst 48:743–761, 1972
14. Becci PJ, McDowell EM, Trump BF: The respiratory epithelium. IV. Histogenesis of epidermoid metaplasia and carcinoma in situ in the hamster. J Natl Cancer Inst 61:577–586, 1978
15. Klein-Szanto AJP: Clear and dark basal keratinocytes in human epidermis. J Cutan Pathol 4:275–280, 1977
16. Klein-Szanto AJP, Olson A, Nettesheim P: Unpublished observations
17. Slaga T, Klein-Szanto AJP: Unpublished observations
18. Prutkin L: Mucous metaplasia and gap junctions in the vitamin A acid-treated skin tumor, keratoacanthoma. Cancer Res 35:364–369, 1975
19. Elias PM, Friend DS: Vitamin-A–induced mucous metaplasia. An in vitro system for modulating tight and gap junction differentiation. J Cel Biol 68:173–188, 1976
20. Trump BF, McDowell EM, Glavin F, Barrett LA, Becci PJ, Schurch W, Kaiser HE, Harris CC: The respiratory epithelium: III. Histogenesis of epidermoid metaplasia and carcinoma in situ in the human. J Natl Cancer Inst 61:563–575, 1978
21. Parmley RT, Spicer SS, Gravin AJ: Multilaminar endoplasmic reticulum and abnormal mitosis in Hodgkin tumor cells. Cancer Res 36:1717–1724, 1976
22. Parkin JL, Brunning RD: Unusual configurations of endoplasmic reticulum in cells of acute promyelocytic leukemia. J Natl Cancer Inst 61:341–348, 1978
23. Schreiber H, Saccomanno G, Martin DH, Brennan L: Sequential cytological changes during development of respiratory tract tumors induced in hamsters by benzo(a)pyrene-ferric oxide. Cancer Res 34:689–698, 1974
24. Saccomanno G, Archer VE, Auerbach O, Saunders RP, Brennan LM: Development of carcinoma of the lung as reflected in exfoliated cells. Cancer 33:256–270, 1974

Acknowledgments

We appreciate the expert technical assistance of Mrs. Alice Pine and Mr. Don Martin and gratefully acknowledge the generous cooperation of Dr. D. C. Swartzendruber, Oak Ridge Associated Universities, who permitted the use of his electron microscope facilities.

Figure 1—Squamous metaplasia with slight atypia. Although a keratinized horny layer is absent, defined stratification can be observed. Note the dark epithelial fusiform cells present in all layers; 200 μg DMBA, 16 weeks. (Toluidine blue, ×480)

Figure 2—Squamous metaplasia with severe atypia. Stratification is still present, but disorganization is also apparent. Great variation in the size and shape of cells and nuclei are evident in all strata; 200 μg DMBA, 16 weeks. (Toluidine blue, ×480)

Figure 3—Squamous metaplasia with moderate atypia. *Arrows* indicate the large number of PAS-positive granules in the epithelium. *HL* = horny layer; 200 μg DMBA, 16 weeks. (PAS, ×480)

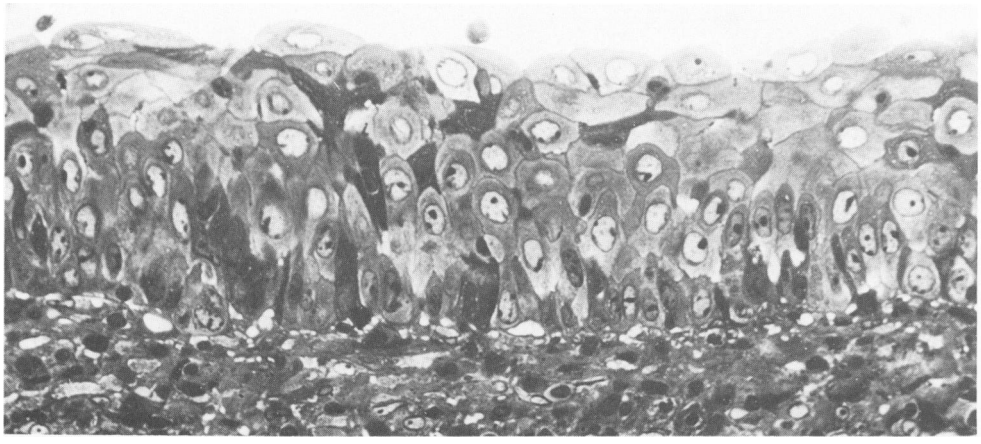

1

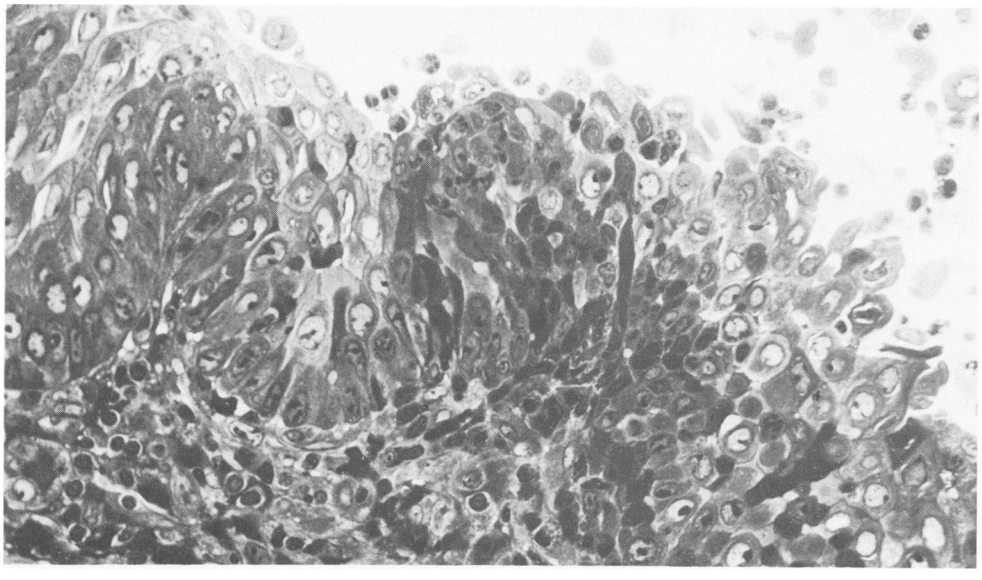

2

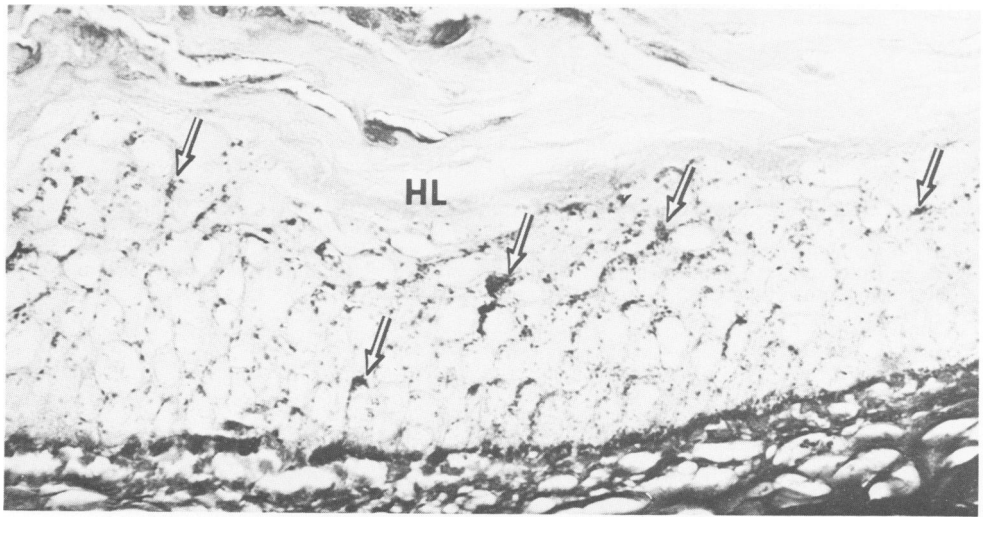

3

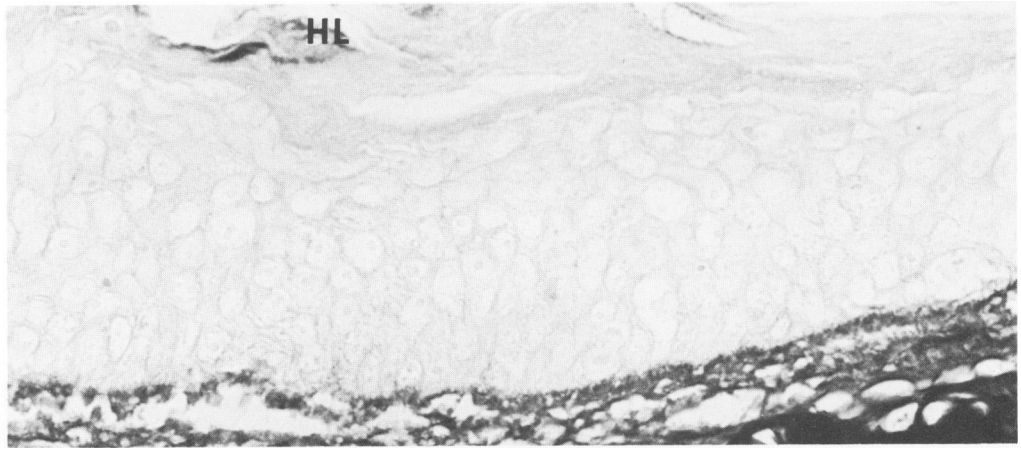

4

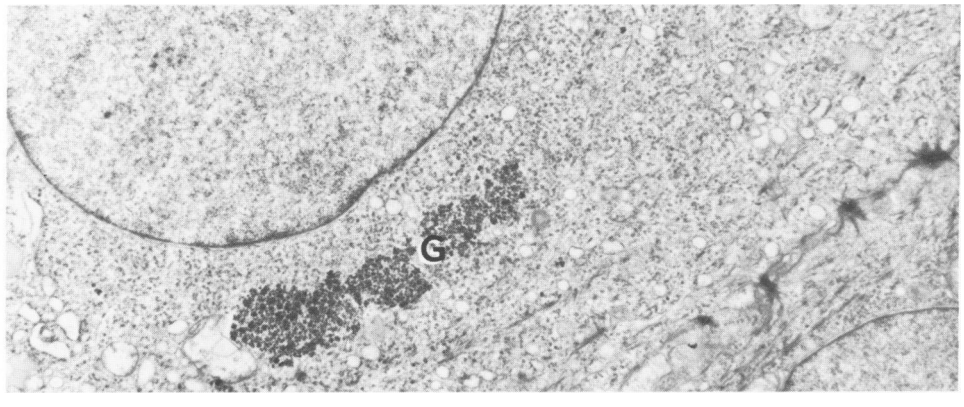

5

Figure 4—Same area as in Figure 3. Note absence of PAS-positive granules. *HL* = horny layer; 200 μg DMBA, 16 weeks. (PAS and amylase, ×480) **Figure 5**—Glycogen particles (*G*) in a spinous cell from lesion similar to Figure 3; 200 μg DMBA, 16 weeks. (×6500) **Figure 6**—Squamous metaplasia with moderate atypia. Granular keratinocyte with a lobulated or fragmented nucleus and zonal condensation of filament bundles (*FB*). *Arrows* indicate the presence of atypical keratohyalin-like material. *KH* = simple keratohyalin granules; 200 μg DMBA, 24 weeks. (×7000) **Figure 7**—Squamous metaplasia with slight atypia. *Arrows* indicate keratohyalin-like material present in close association with the cytoplasmic membrane; 200 μg DMBA, 16 weeks. (× 14,000)

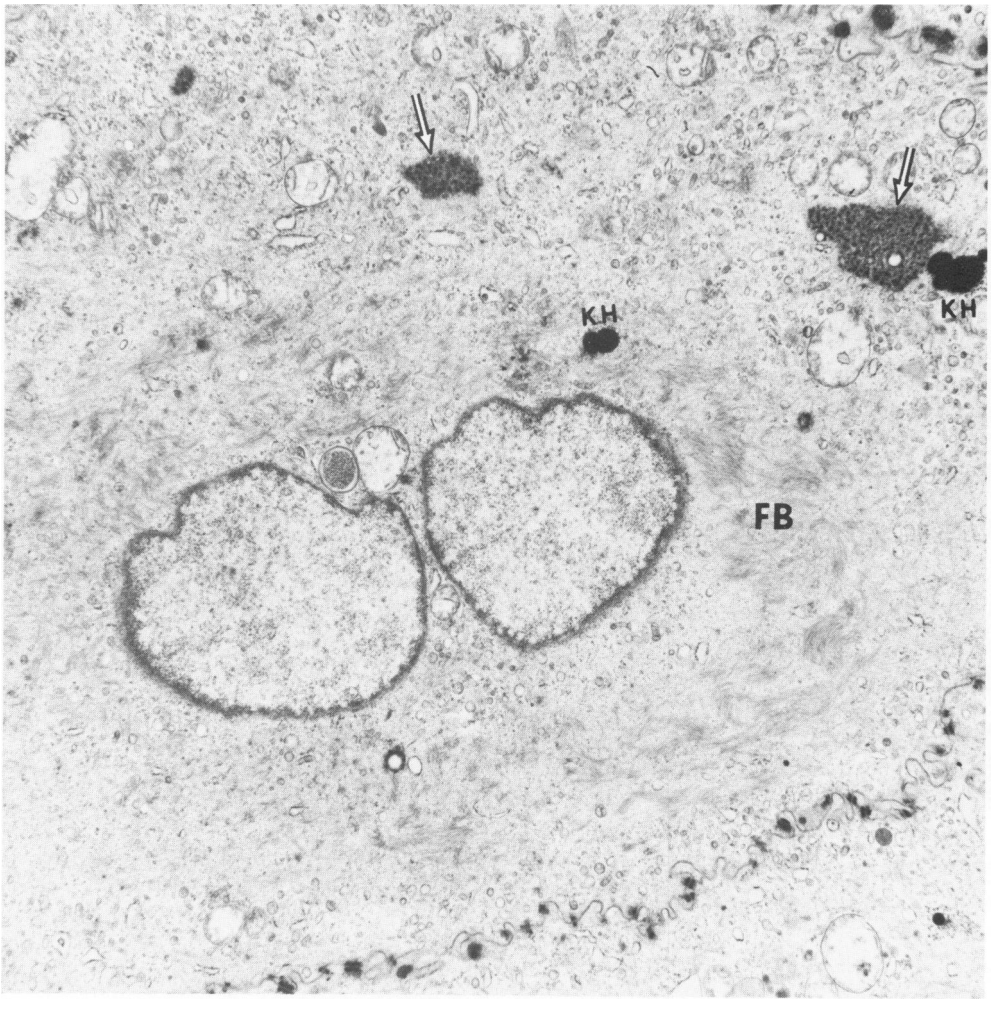

6

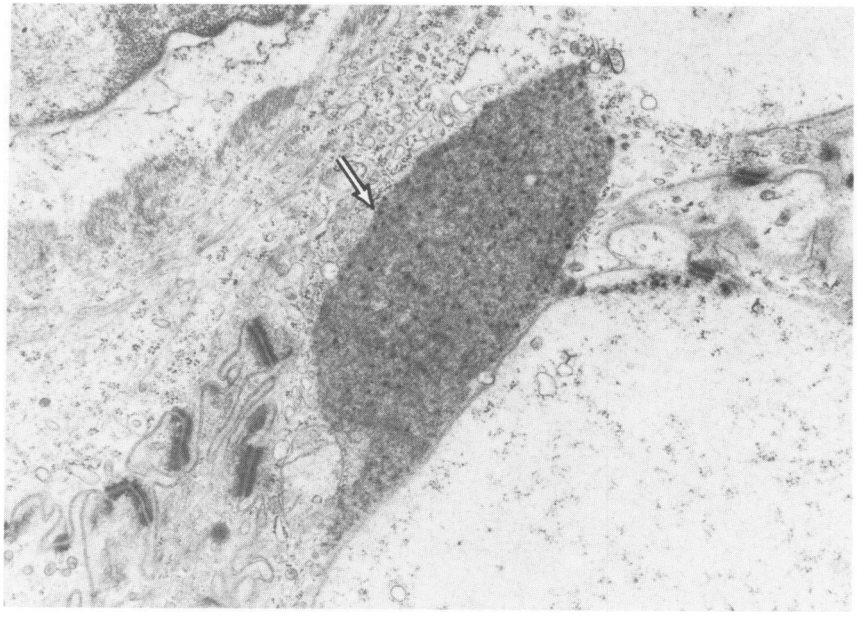

7

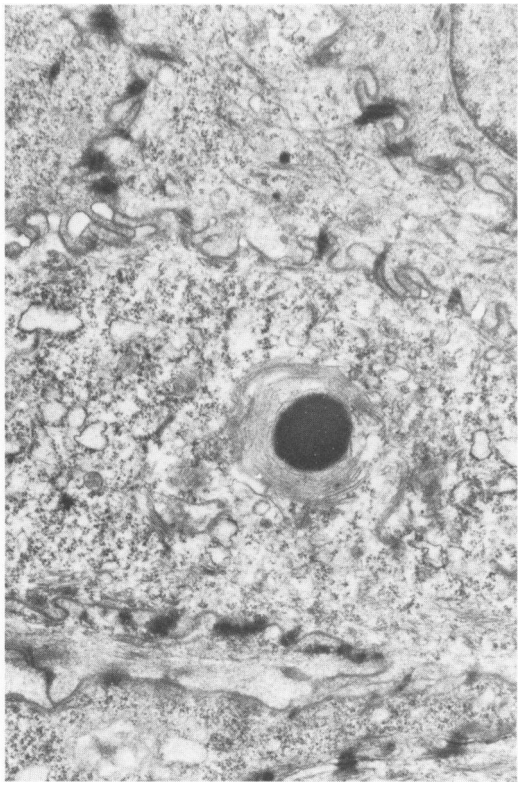

Figure 8—Squamous metaplasia with moderate atypia. Atypical keratohyalin granule surrounded by concentric array of membranous structures; 200 μg DMBA, 12 weeks. (×9000) **Figure 9**—Squamous metaplasia with severe atypia. Basal cell with extremely pleomorphic mitrochondria. Note the direct contact of collagen fibers (*C*) with an epithelial cell (*arrows*) and the presence of alternating areas in which the basal lamina is still evident. *H* = hemidesmosomes; 200 μg DMBA, 24 weeks. (×9500) **Figure 10**—Squamous metaplasia with severe atypia. Dark epithelial cell surrounded by clear epithelial cells in the suprabasal region of the spinous layer; 200 μg DMBA, 16 weeks. (×7500) **Figure 11**—Carcinoma *in situ*. *Arrows* indicate the presence of microcysts; 200 μg DMBA, 24 weeks. (H&E, ×400)

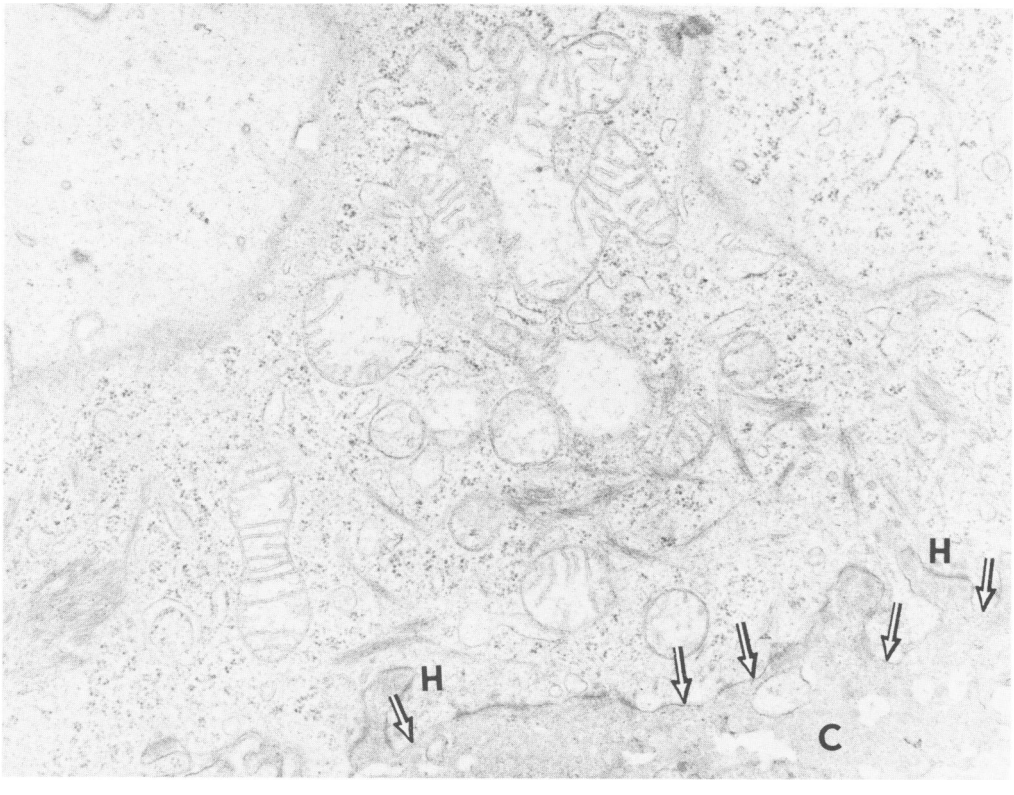

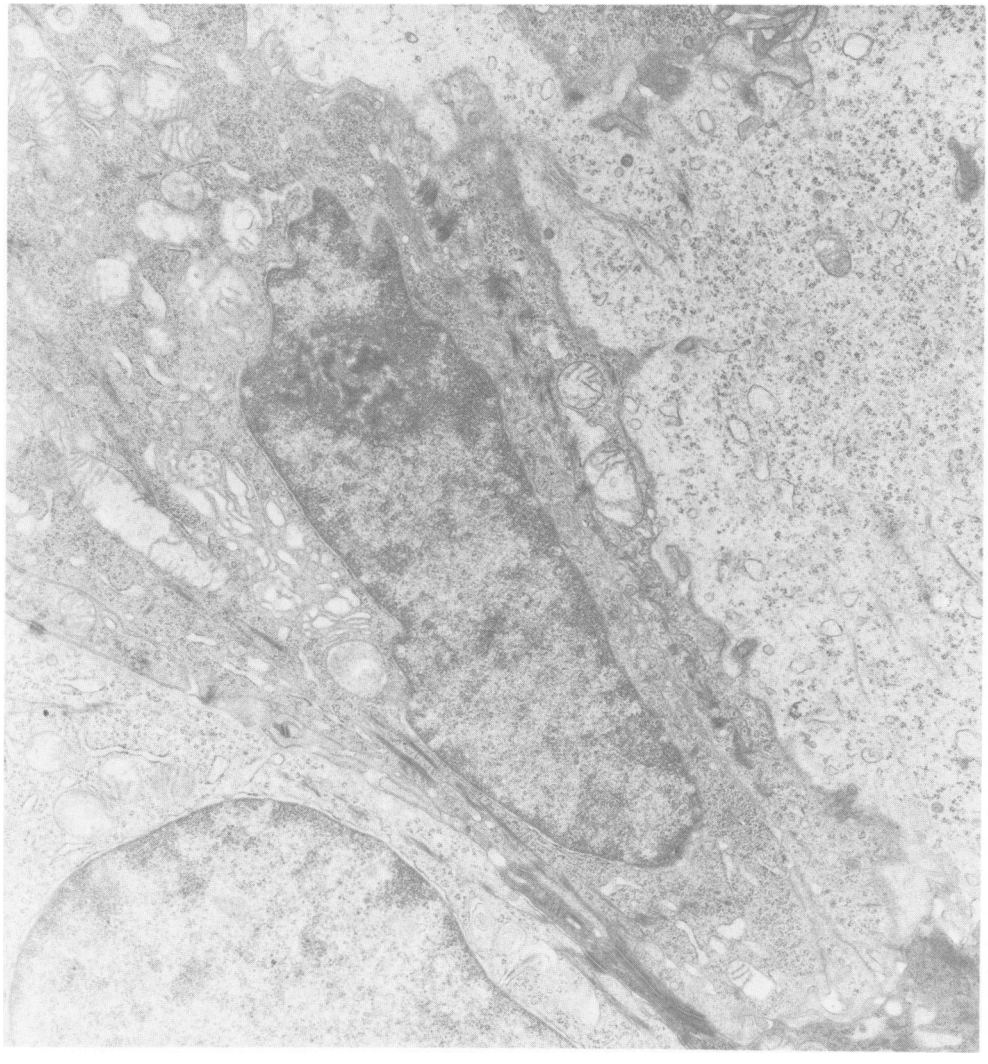

10

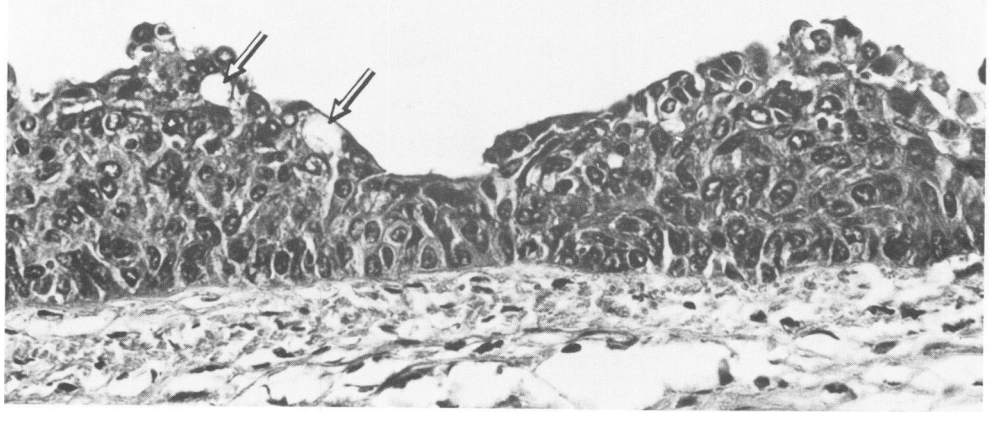

11

12

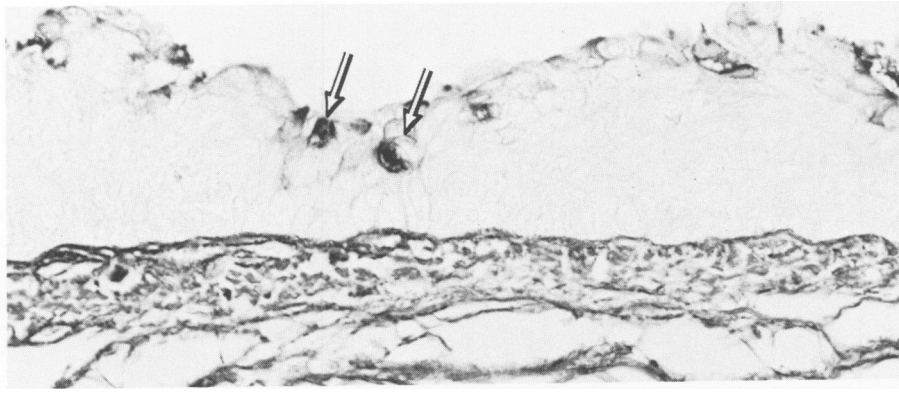

13

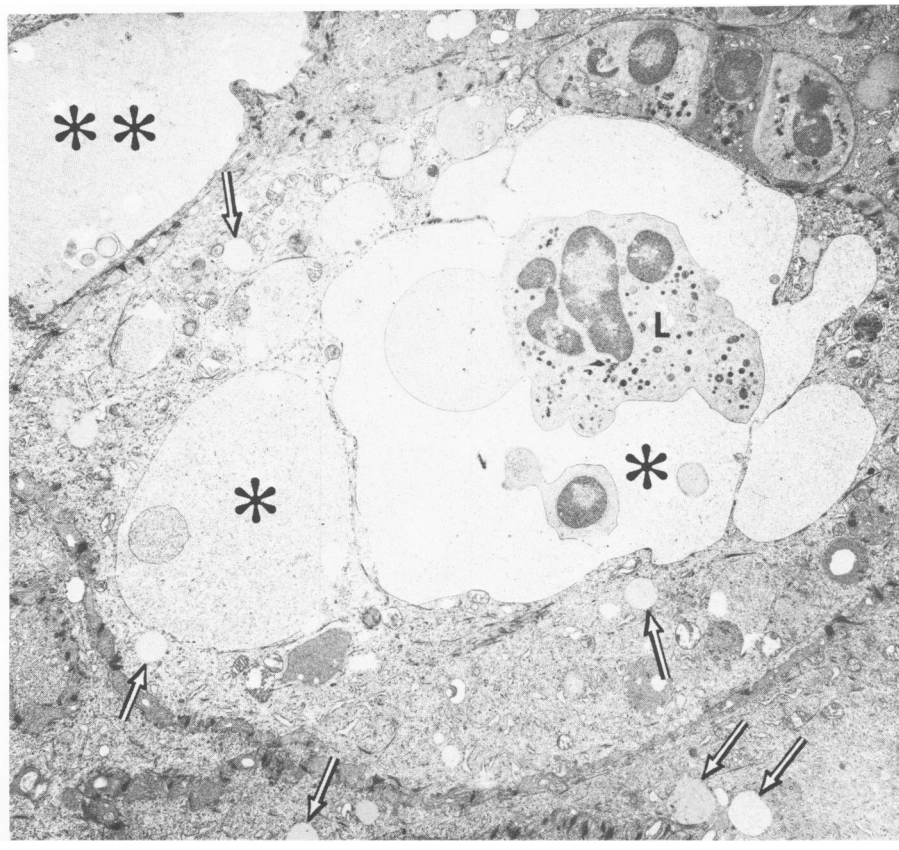

Figure 12—Carcinoma *in situ*. *Arrows* indicate microcysts with an accumulation of acid mucosubstances in same area as shown in Figure 11. (PAS–AB, pH 2.6, ×400) **Figure 13**—Carcinoma *in situ*. Numerous microcysts, one intercellular (**) and several apparently in an intracellular position (*). Note the finely granular material of variable electron density in the microcysts' lumens. Numerous cytoplasmic bodies compatible with secretory droplets (*arrows*) are seen. *L* = leucocyte with blebbing cytoplasm; 200 μg CMBA, 16 weeks. (×4200) **Figure 14**—Carcinoma *in situ*. Total cell dyskeratosis, with numerous condensed filament bundles (*FB*) and rests from nuclear structures (*N*). The basal lamina is not visible and the cell is in direct contact with collagen fibers (*arrows*); 200 μg DMBA, 16 weeks. (×7500) **Figure 15**—Carcinoma *in situ*. Presence of a dark epithelial cell in the superficial layer; 200 μg DMBA, 24 weeks. (×4200)

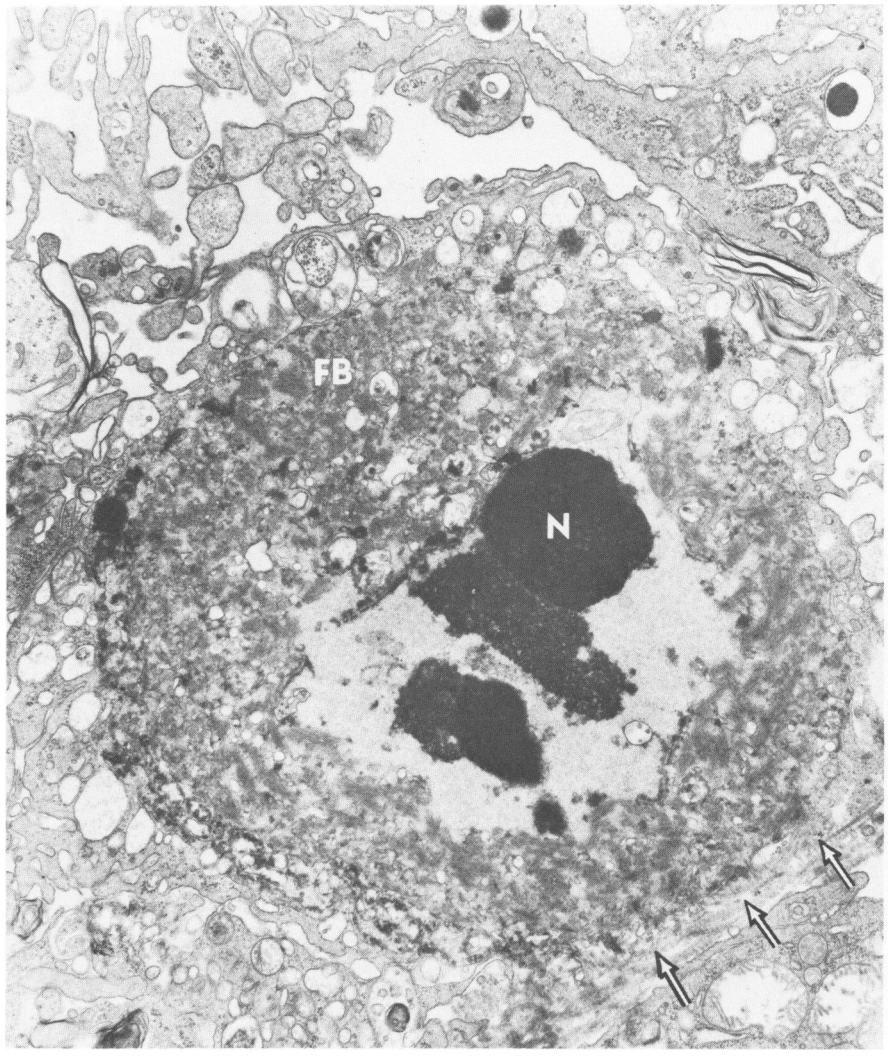

14

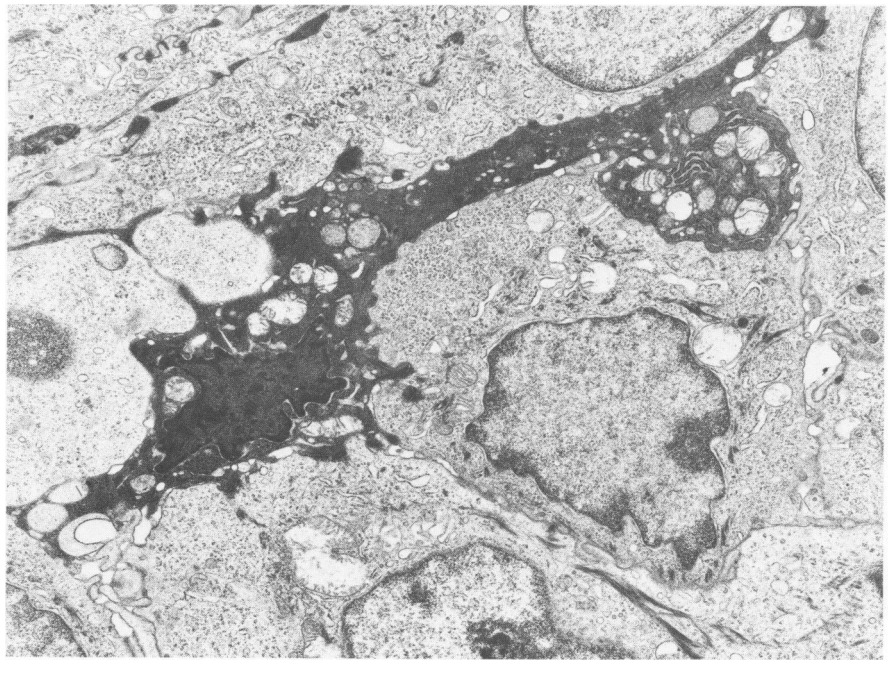

15

16

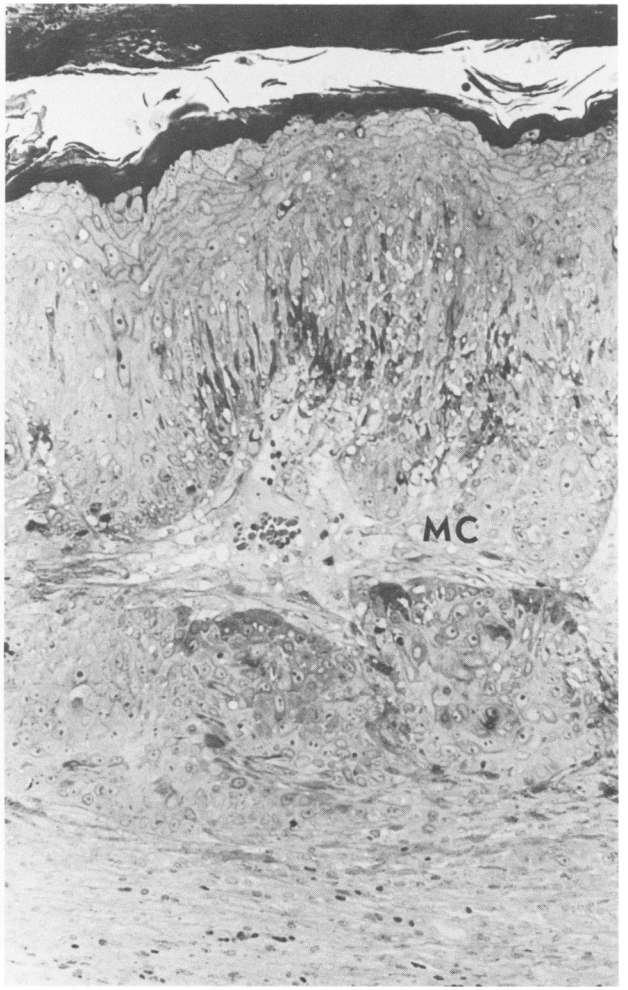

17

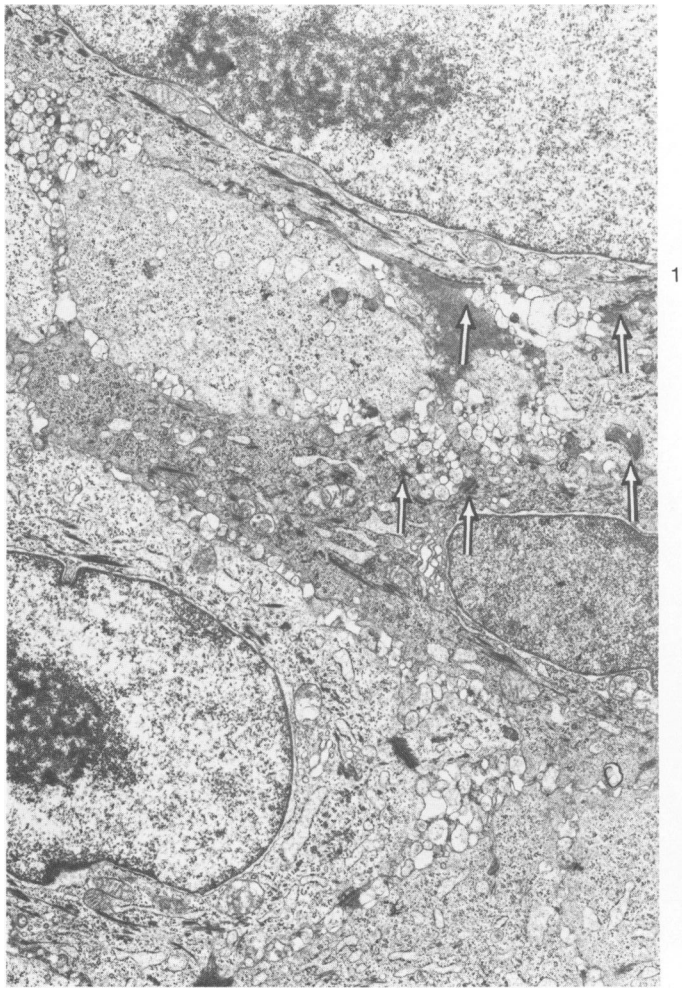

Figure 16—Squamous metaplasia with moderate atypia showing direct spatial relation with areas of microinvasive carcinoma (*MC*) and deeper carcinomatous invasion; 200 μg DMBA, 48 weeks. (Toluidine blue, ×200) **Figure 17**—Microinvasive squamous carcinoma. Note presence of dark and clear epithelial cells, as well as production of basal lamina-like material between cells. Numerous hemidesmosomes are to be found in the same areas (*arrows*); 200 μg DMBA, 48 weeks. (×5000)

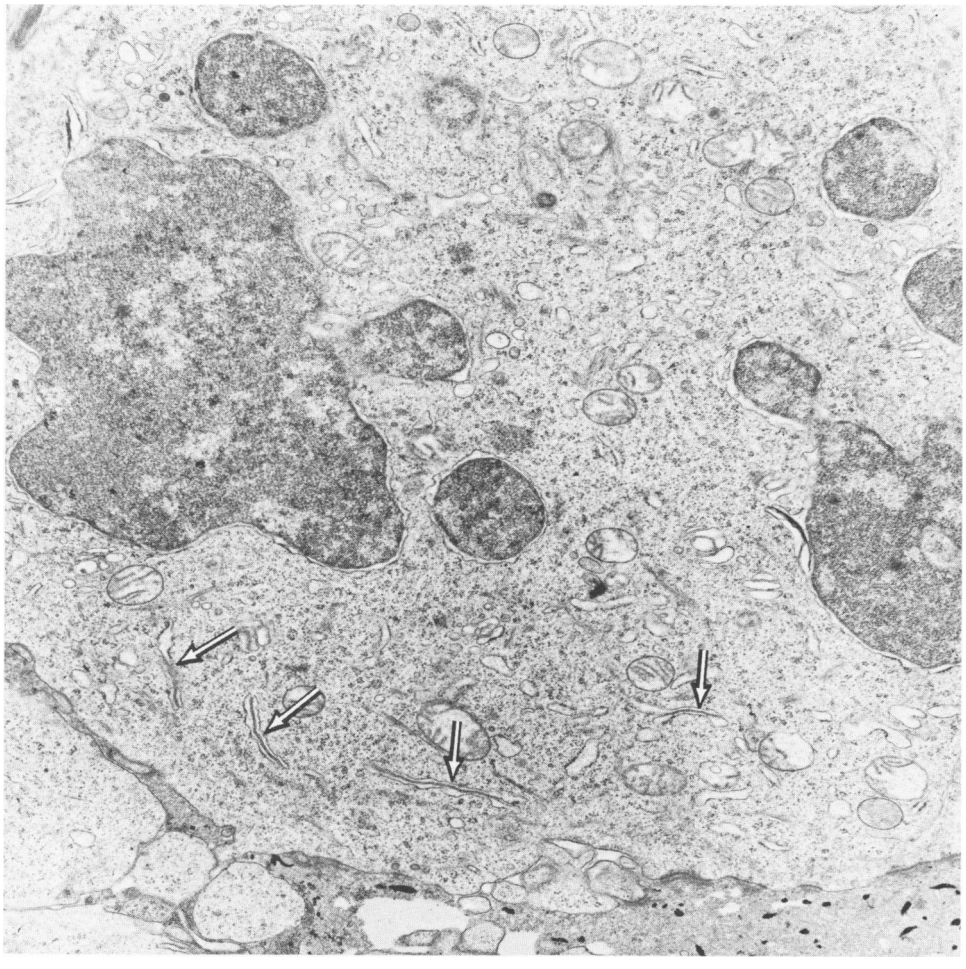

Figure 18—Microinvasive carcinoma. Carcinoma cell with lobulated or fragmented nucleus and numerous multilaminar endoplasmic reticulum profiles (*arrows*); 200 μg DMBA, 48 weeks. (×7500)

[*End of Article*]